

## Weak localization in pregraphitic carbon fibers

V. Bayot, L. Piraux, J.-P. Michenaud, and J.-P. Issi

*Unité de Physico-Chimie et de Physique des Matériaux, Département des Sciences des Matériaux et des Procédés, Université Catholique de Louvain, place Croix du Sud, 1 B-1348 Louvain-la-Neuve, Belgium*

(Received 18 January 1989)

High-resolution resistivity and magnetoresistance measurements have been performed as a function of temperature on pregraphitic carbon fibers. The resistivity exhibits a negative temperature coefficient ( $d\rho/dT < 0$ ) from room temperature down to 1.5 K. It is shown that such behavior can hardly be explained by a thermal excitation of carriers in the liquid-helium temperature range within the framework of the simple two-band model, usually applied to graphitic and pregraphitic structures. The magnetoresistance presents a negative component more pronounced at low temperature. It is found that the magnetic field acts to restore the expected behavior of the resistivity in the low-temperature range, in the sense that the resistivity becomes gradually temperature independent. These observations as well as the experimental results obtained at higher temperature are consistent with the weak-localization theory for two-dimensional systems.

### I. INTRODUCTION

Negative magnetoresistances in pregraphitic carbons were first reported in 1956 by Mrozowski and Chaberski.<sup>1</sup> Since that time, this unusual phenomenon has been observed in various kinds of poorly graphitized carbon materials,<sup>2-6</sup> as well as in polyacrylonitrile (PAN)-derived fibers,<sup>7</sup> pitch-based fibers,<sup>8-10</sup> and benzene-derived fibers (BDF).<sup>11,12</sup>

Among the several models that have been proposed to explain this peculiar behavior, the Bright model<sup>13</sup> has received a great deal of attention in the last decade. That model is based on the increase in carrier density with magnetic field. Bright argued that, for turbostratic graphite, the electronic structure should be nearly that of two-dimensional graphite. Under this assumption, the density of states in a magnetic field is represented by  $\delta$  functions which are broadened in the presence of defect scattering, with the quantum limit occurring at very low magnetic fields. The free carriers lie in the first Landau level and the increase of the density of states and carrier density with magnetic field results in a negative magnetoresistance. This model worked quite well in explaining a lot of data available at that time. However, recent experimental data<sup>10,12</sup> suggests that this model cannot account for all the observed phenomena. For example, it is not able to explain the marked temperature dependence of the magnetoresistance below liquid-helium temperature nor the absence of saturation of the magnetoresistance at high magnetic fields. In order to take into account these experimental observations, additional mechanisms combining a magnetic-field-dependent ionized-impurity-scattering process and the electron-Rayleigh-wave interaction<sup>12,14</sup> have been recently proposed as an extension of the Bright model.

On the other hand, some authors have recently proposed a different approach based on localization effects associated with weakly disordered electronic systems

(“weak localization”) to explain the negative magnetoresistance in Grafoil<sup>15</sup> and in PAN-derived carbon fibers.<sup>16</sup> The weak-localization phenomenon is an inherent interference effect common to any wave propagation in a disordered medium.<sup>17-19</sup> In disordered electronic systems, the weak-localization effect occurs when the probability for “elastic” scattering of carriers by static lattice defects is much larger than that for the temperature-dependent “inelastic” scattering processes due to carrier-phonon and carrier-carrier interactions. As a result, the weak-localization effect is generally a low-temperature effect. If  $\tau_0$  and  $\tau_i$  are elastic and inelastic relaxation times, respectively, the initial condition for the occurrence of such a phenomenon is that  $\tau_0 \ll \tau_i$ . Using time-reversal symmetry, it was demonstrated that constructive interference of the elastically scattered partial electron waves takes place in the backward direction, leading to an enhanced backscattering probability. This effect gives rise to a small electrical resistivity increase with decreasing temperature, which is the prominent feature of the weak-localization phenomenon. Since the magnetic field tends to suppress the phase coherence of the backscattered waves, it destroys the localization effect. Therefore, the magnetoresistance is negative and its absolute value increases as the temperature decreases. Figure 1 illustrates schematically the basic differences between the Bright model and the weak-localization approach. The theory of weak localization has been extended to include other effects such as spin-orbit coupling and magnetic impurity scattering<sup>19</sup> and is also applicable to systems with more than one type of carrier.<sup>20</sup> Different temperature dependences are expected according to the dimensionality of the electron system. For two-dimensional systems, the theory predicts a logarithmic temperature dependence of the resistivity correction when spin-dependent mechanisms are negligible. A considerable number of experimental observations have been reported in various systems in the last few years. (For re-

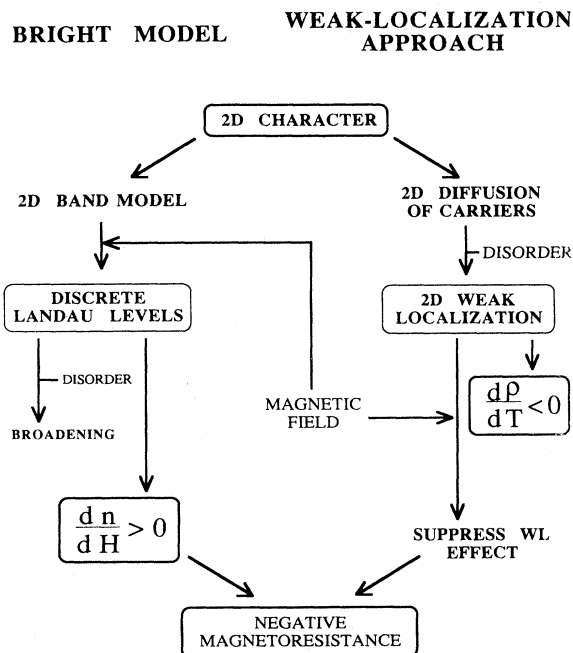


FIG. 1. Schematic diagram showing the basic differences between the Bright model and the weak-localization approach for explaining negative magnetoresistance in pregraphitic materials.

view papers, see Refs. 18, 21, and 22).

More recently, it was shown that acceptor-graphite intercalation compounds constitute an attractive class of materials to investigate weak-localization effects in the two-dimensional regime. A logarithmic increase of resistance with decreasing temperature and a negative magnetoresistance have been observed on a set of low-stage acceptor-graphite-fiber intercalation compounds with different host-graphite materials and intercalates in the low-temperature range.<sup>23-25</sup> In that case, however, it was demonstrated that the disorder-enhanced carrier-carrier Coulomb interaction contributes largely to the logarithmic resistance correction.

In this paper, we report highly accurate resistivity and magnetoresistance measurements performed on pitch-based, PAN-based, and benzene-derived carbon fibers. From these results it appears that the electrical resistivity of pregraphitic carbon fibers displays another anomalous behavior: the temperature coefficient of the resistivity remains negative down to the lowest temperature investigated i.e., 1.5 K. Using the simple two-band (STB) model developed by Klein<sup>26</sup> and assuming that the carrier mobility is temperature independent at low temperature, we show that such a behavior cannot be ascribed to the thermal excitation of the charge carriers. The data obtained with the magnetic field applied perpendicular to the fiber axis show that the magnetic field acts to suppress this anomalous behavior. Thus, the negative magnetoresistance phenomenon can be understood as a process which tends to restore an expected low-temperature behavior of the resistivity. The weak-

TABLE I. Electrical characteristics of the fibers investigated.

	$\rho(4.2 \text{ K})$ ( $10^{-8} \Omega \text{ m}$ )	$\rho_{300 \text{ K}}/\rho_{4.2 \text{ K}}$
GY-70	902	0.763
BDF2000	801	0.765
P55	798	0.782
P100	683	0.479
VSC25	421	0.476
P100-4	357	0.539
P120	313	0.519

localization theory for two-dimensional systems is shown to be relevant for quantitatively explaining both the resistivity and magnetoresistance data as a function of the temperature and magnetic field.

## II. EXPERIMENT

Resistivity and magnetoresistance measurements of several pitch-based carbon fibers produced by Amoco (P55, VSC25, P100, P100-4, and P120), a PAN-based carbon fiber (GY-70), and a 2000°C heat-treated benzene-derived fiber (BDF2000) have been performed using a classical dc four-probe method between 1.5 and 300 K. Magnetic fields up to 1 T were provided by means of a classical electromagnet. The current flowing in the single fibers was provided by a high-stability Keithley K224 current source and the input power was kept to less than  $10^{-8}$  W to avoid self-heating. The output voltage was obtained accurately by means of a Keithley K181 nanovoltmeter, which could resolve  $10^{-8}$  V. For each sample, the electrical resistance was measured with a resolution of a few parts in  $10^5$ . The fibers were mounted with their axis perpendicular to the applied magnetic field and electrical contacts were ensured by means of platinum paste.

The values of the resistivity at liquid-helium temperature and that of the residual resistance ratio  $\rho_{300 \text{ K}}/\rho_{4.2 \text{ K}}$  for each fiber are given in Table I. For the BDF2000, P55, and GY-70 samples, the interlayer spacing is approximately 3.42 Å (Refs. 27 and 28) which is characteristic of a turbostratic arrangement of the planes.<sup>26</sup> For the other samples the interlayer spacing is about 3.37 Å,<sup>28,29</sup> which is an intermediate value between that of the graphitic and the turbostratic structures.

## III. RESULTS

The low-temperature dependences of the zero-field electrical resistivities are shown in Fig. 2. All carbon fibers exhibit an increase in resistivity with decreasing temperature though the resistivity values are different. These data are in good agreement with those reported previously by several authors.<sup>9,27</sup> At 4.2 K, the P120 and the GY70 fibers show the lowest and highest values of resistivity, respectively. The resistivity increases monotonically as the temperature decreases down to the lowest temperature investigated, i.e.,  $d\rho/dT$  is always negative whatever the temperature range considered. Such a behavior is in contrast to that presented by more graphi-

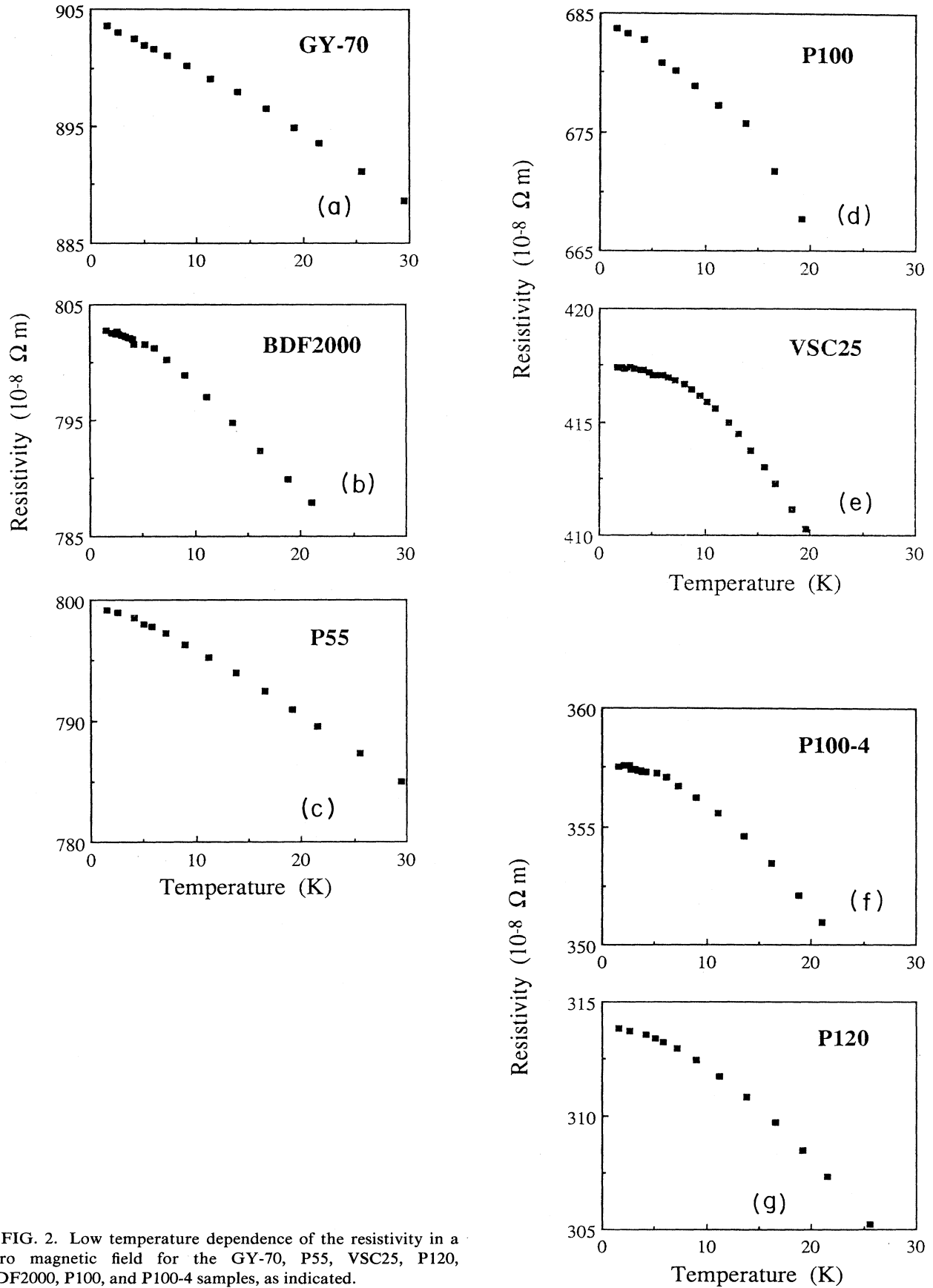


FIG. 2. Low temperature dependence of the resistivity in a zero magnetic field for the GY-70, P55, VSC25, P120, BDF2000, P100, and P100-4 samples, as indicated.

tized fibers<sup>11,30,31</sup> for which a maximum is observed in the resistivity, in the range 20–60 K, followed by a decrease of resistivity with decreasing temperature so that a positive temperature coefficient of resistivity takes place in the lowest-temperature range. An interpretation of the observed temperature variation of the zero-field electrical resistivity of carbon fibers for different heat-treatment temperatures (HTT) has previously been proposed, taking into account the expected temperature dependence of

both the carrier densities and mobilities in these materials.<sup>27,31</sup>

The magnetoresistance has been measured over a wide temperature range (1.5–300 K) with the magnetic field perpendicular to the fiber axis. While at low temperatures each sample exhibits a negative magnetoresistance, some differences appear at higher temperature, as illustrated in Fig. 3 for three types of fibers. For the BDF2000, the magnetoresistance remains negative up to

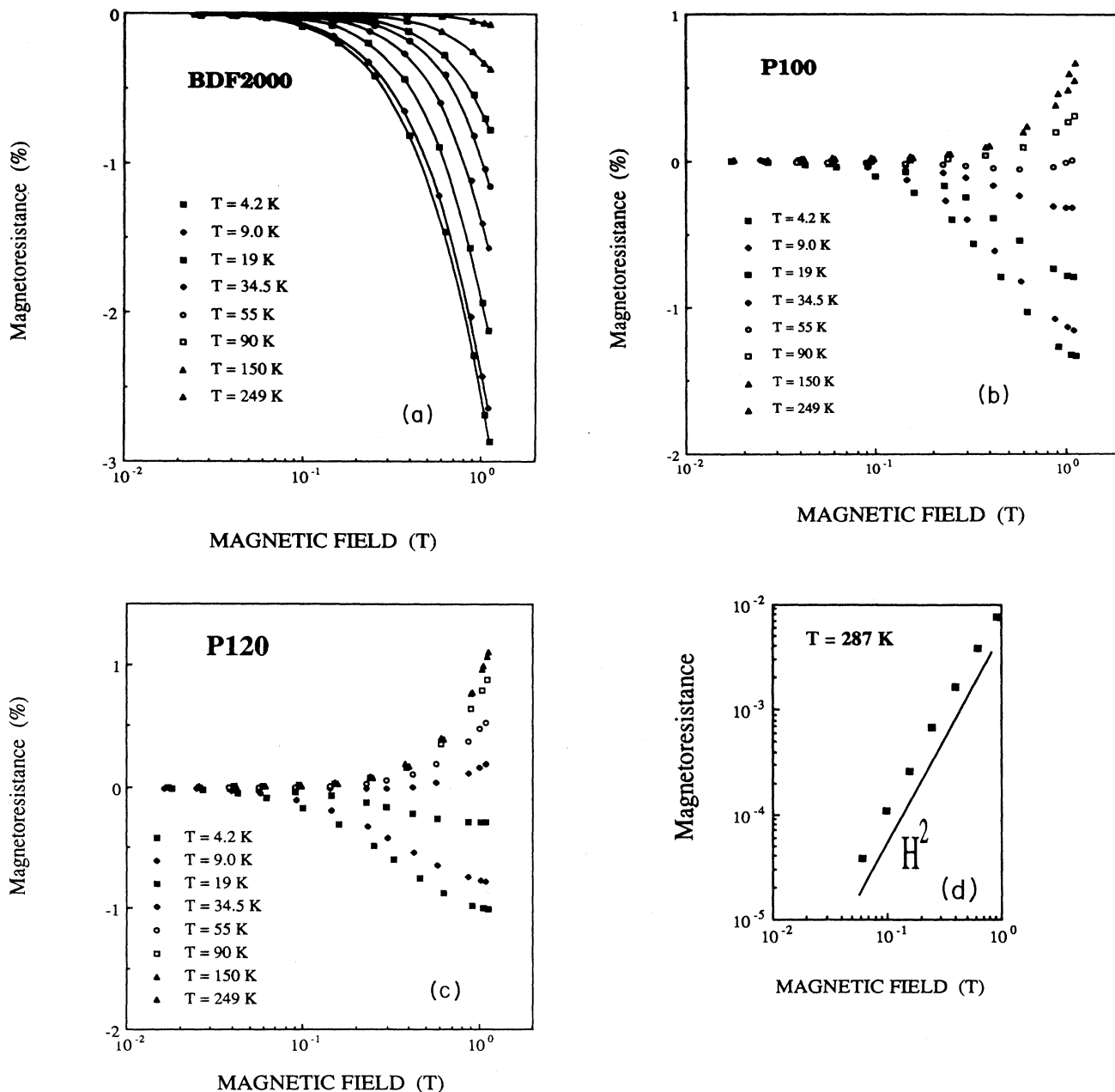


FIG. 3. Magnetoresistance of (a) BDF2000, (b) P100, and (c) P120 samples in magnetic field perpendicular to the fiber axis at several temperatures, as indicated. In (a), lines are guides for the eyes. Figure 3(d) shows the  $H^2$  dependence of the room-temperature magnetoresistance at low magnetic field for the P120 sample.

room temperature, though the absolute value decreases with increasing temperature. For the P100 and P120 fibers, on the other hand, positive values due to the Lorentz force are observed above a certain temperature, which depends on the carbon fiber considered. Our results indicate that the lower the residual resistivity, the lower the temperature at which the magnetoresistance becomes positive. As shown in Fig. 3(d), the low-field magnetoresistance follows an  $H^2$  dependence at room temperature, in agreement with previous results.<sup>5,6,26,31</sup> Also, for a given magnetic field intensity, the measured magnetoresistance values around room temperature are different from one type of fiber to another. Such differences in the high-temperature results are indicative of differences in the carrier mobilities corresponding to the degree of disorder in a sample. The results obtained on the GY70, P55, VSC25, and P100-4 samples are not shown in Fig. 3. The first two exhibit the same behavior as the BDF2000 sample, while the last two exhibit the same behavior as the P100 and P120 samples. For the BDF2000, P100, P100-4, and P120 samples, our data are in good agreement with those found elsewhere.<sup>9,10,12</sup>

#### IV. DISCUSSION

##### A. Temperature and field dependence of the resistivity

We first consider the zero-field temperature dependence of the electrical resistivity, as well as the effect of a magnetic field on the low-temperature dependence. For each fiber, the carrier scattering is dominated by collisions with static defects in the low-temperature range. If we assume that the carrier mobility is temperature independent below and around liquid-helium temperature, the observed variation should be attributed to the variation of the density of carriers. In the simple two-band model, the ratio of the carrier density at temperature  $T$  to that at  $T=0$  K is given by<sup>7</sup>

$$F(T) = \frac{n(T)}{n(T=0 \text{ K})} = \frac{k_B T}{\epsilon_0 - \epsilon_i} \times \left\{ \ln \left[ 1 + \exp \left[ \frac{\epsilon_F}{k_B T} \right] \right] + \ln \left[ 1 + \exp \left[ \frac{\epsilon_0 - \epsilon_F}{k_B T} \right] \right] \right\}, \quad (1)$$

where  $\epsilon_0$  is the energy-band overlap,  $\epsilon_F$  is the Fermi energy measured from the bottom of the conduction band, and  $\epsilon_i = \epsilon_F$  or 0 according to whether the Fermi energy is negative or positive. From this relation, it may be easily calculated that  $dF/dT = -\rho^{-1} d\rho(T)/dT$  at 4.2 K is less than  $10^{-7} \text{ K}^{-1}$  whatever reasonable values are assumed for the Fermi energy and the band overlap, so that the carrier density is expected to be quasi-temperature-independent around liquid-helium temperature. It should be noted that in relation (1) both  $\epsilon_0$  and  $\epsilon_F$  are ex-

pected to be temperature independent, which could be strictly correct only in the liquid-helium temperature range. The zero-field resistivity results shown in Fig. 4 indicate clearly that the experimental resistivity slope (between  $3 \times 10^{-4}$  and  $6 \times 10^{-4} \text{ K}^{-1}$ ) is much more pronounced than the theoretical prediction of relation (1). One concludes that the observed increase in resistivity as the temperature is lowered cannot be associated with the charge-carrier variation predicted within the framework of the simple two-band model.

As we increase the external magnetic field, we observe that the temperature dependence of the resistivity becomes gradually compatible with that predicted by the STB model, in the sense that the resistivity becomes gradually temperature independent with increasing value of magnetic field. This observation suggests that the magnetic field acts to destroy an extra mechanism contributing to the resistivity. This point of view is in opposition to the Bright approach, which invokes a field-induced mechanism to explain the negative magnetoresistance phenomenon.

##### B. The weak-localization interpretation

We now discuss these anomalous temperature and magnetic field dependences of the resistivity observed in pregraphitic fibers in terms of the weak-localization phenomenon. Such a phenomenon occurs in weakly disordered systems and gives rise to an extra resistivity at low temperature as well as to a negative magnetoresistance. It occurs whatever the dimensionality of the electronic system, but owing to the turbostratic structure of the pregraphitic carbon fibers,<sup>7,13,26</sup> the two-dimensional weakly disordered regime seems more appropriate. Our approach is thus different from that used by Koike *et al.*,<sup>15</sup> who discussed their results obtained on Grafoil in terms of weak localization in the three-dimensional regime.

In the absence of spin-dependent scattering processes, two-dimensional (2D) weak localization normally leads to a logarithmic increase of the resistivity as the temperature is lowered; this is different from what we observe in our experiments. However, it is well established that scattering by magnetic impurities and spin-orbit coupling may cause significant changes in the temperature-dependent correction term to the resistance. Indeed, the inclusion of magnetic impurity scattering may lead to a low-temperature saturation of the resistivity, while a sufficiently strong spin-orbit coupling changes localization into "antilocalization," i.e., a decreasing resistance as the temperature is lowered and a positive magnetoresistance.

We first consider the magnetoresistance results since quantitative informations can be obtained on the magnitude of such spin-dependent processes as well as on the carrier inelastic scattering mechanisms. In the two-dimensional regime, the correction to the sheet conductance  $G$  produced with the magnetic field  $H$  oriented perpendicular to the plane of the 2D carrier system is given by<sup>19,32</sup>

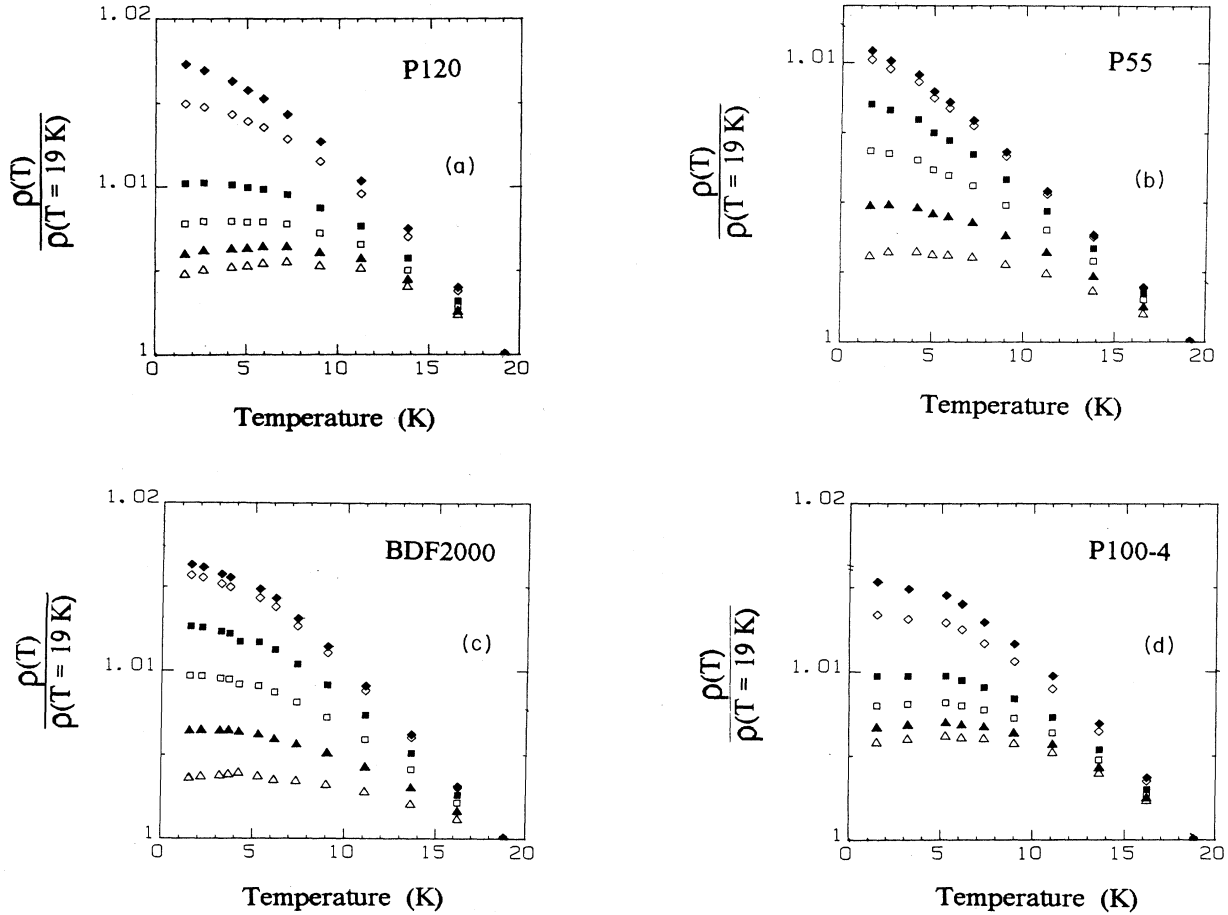


FIG. 4. Influence of magnetic fields on the low-temperature resistivity of pregraphitic carbon fibers, as indicated. The applied fields are 0 T ( $\blacklozenge$ ), 0.1 T ( $\diamond$ ), 0.3 T ( $\blacksquare$ ), 0.5 T ( $\square$ ), 0.8 T ( $\blacktriangle$ ), and 1.2 T ( $\triangle$ ).

$$G(H, T) = G_0 + \frac{e^2}{2\pi^2\hbar} \left[ -\Psi \left[ \frac{1}{2} + \frac{H_1}{H} \right] + \frac{3}{2} \Psi \left[ \frac{1}{2} + \frac{H_2(T)}{H} \right] - \frac{1}{2} \Psi \left[ \frac{1}{2} + \frac{H_3(T)}{H} \right] \right]. \quad (2)$$

Here  $G_0$  is the sheet conductance as calculated in the classical Boltzmann formulation of the transport theory; in the special case of a film as quasi-2D system, the sheet conductance is the product of the 3D conductivity by the thickness of the film. In Eq. (2),  $\Psi$  is the digamma function and  $H_1$ ,  $H_2(T)$ , and  $H_3(T)$  are defined by

$$\begin{aligned} H_1 &= H_0 + H_{s.o.} + H_s, \\ H_2(T) &= H_i(T) + \frac{4}{3} H_{s.o.} + \frac{2}{3} H_s, \\ H_3(T) &= H_i(T) + 2H_s, \end{aligned}$$

where the quantities

$$H_k = \frac{\hbar}{4eD\tau_k} \quad (k=0, i, s, s.o.) \quad (3)$$

represent the characteristic fields associated with the scattering mechanism  $k$  standing for elastic scattering (0), inelastic scattering (i), magnetic impurity scattering (s), or spin-orbit coupling (s.o.);  $\tau_k$  is the relaxation time corresponding to the scattering type  $k$ ,

$$D = \frac{1}{2} v_F^2 \tau_0 \quad (4)$$

is the 2D diffusion constant, and  $v_F$  is the Fermi velocity.

In the limit of zero magnetic field, Eq. (2) becomes

$$G(0, T) = G_0 + \frac{e^2}{2\pi^2\hbar} \ln \left[ \frac{H_2^{3/2}}{H_1 H_3^{1/2}} \right]. \quad (5)$$

For convenience, we discuss our results in terms of the magnetoresistance  $\Delta R/R$  rather than in terms of the magnetoconductance  $\Delta G/G$  where  $\Delta G = G(H, T) - G(0, T)$ . Since  $\Delta G/G \ll 1$ , we have  $\Delta R/R \cong -\Delta G/G$ . Also, we introduce the sheet resistance  $R_\square = 1/G_0$ .

The above relations are strictly valid only when the magnetic field is perpendicular to the 2D carrier system which lies here in the graphite layers. Since the magnetic field is applied perpendicularly to the fiber axis, we have to consider the arrangement of the graphite planes around the fiber axis. The graphitic planes present different orientations with respect to the magnetic field direction and the electrical transport in the planes will be mostly affected by the perpendicular component of the field. So, the effective magnetic field acting on the charge carriers is different in different planes. Information on the organization of the graphite layers can be obtained from angular dependence measurements of the magnetoresistance. In agreement with previous results,<sup>30</sup> we found no significant angular dependence, suggesting that the planes are uniformly distributed around the fiber axis. This result also indicates the poor degree of crystalline orientation in our samples. The large anisotropy in the negative magnetoresistance observed in pyrolytic graphites<sup>4,6</sup> allows us to assume that only the magnetic field component perpendicular to the planes is responsible for the magnetoresistance. Therefore, the apparent magnetoresistance, i.e., the experimental magnetoresistance  $[\Delta R(H, T)/R(0, T)]_{\text{expt}}$  is given by<sup>25</sup>

$$\left[ \frac{\Delta R(H, T)}{R(0, T)} \right]_{\text{expt}} = \frac{1}{\pi} \int_{-\pi/2}^{\pi/2} \left[ \frac{\Delta R(H \cos\theta, T)}{R(0, T)} \right]_{\text{theor}} d\theta, \quad (6)$$

where  $\theta$  is the angle between the normal to a graphite layer and the magnetic field direction. The theoretical magnetoresistance which appears under the integral is the one that would be observed if the magnetic field were perpendicular to each graphite layer.

For some samples, we had to split the experimental magnetoresistance into the classical positive magnetoresistance component due to the Lorentz force and the negative magnetoresistance that we assume to be associated with the weak-localization effect. This positive magnetoresistance is quite apparent in the P100, VSC25, P100-4, and P120 fibers, but does not show up in the other fibers, which are more disordered. The total measured magnetoresistance is thus the sum of two terms,

$$(\Delta R/R)_{\text{expt}} = (\Delta R/R)_{\text{Lorentz}} + (\Delta R/R)_{\text{weak loc}}. \quad (7)$$

As a first approximation, owing to the geometrical layout of the graphite planes around the fiber axis, the positive contribution to the low-field magnetoresistance takes the following form:<sup>31</sup>

$$(\Delta R/R)_{\text{Lorentz}} \cong \frac{1}{2}(\mu H)^2, \quad (8)$$

where the in-plane mobility  $\mu$  is determined by the combination of two relaxation processes<sup>28</sup>—phonons and defects. The Matthiessen's law implies for the total mobility the usual form

$$1/\mu = 1/\mu_0 + 1/\mu_i, \quad (9)$$

where  $\mu_0$  corresponds to defect scattering and  $\mu_i$  to scattering by phonons. In order to separate the Lorentz

component from the weak-localization component over a wide temperature range we make the following assumptions. (i) At room temperature, the negative contribution to the measured magnetoresistance due to weak localization is negligible and  $(\Delta R/R)_{\text{expt}}$  corresponds exactly to the Lorentz contribution as given by expression (8). (ii) Up to room temperature, the mobility is largely limited by impurity and defect scattering so that  $\mu \approx \mu_0$  and  $(\Delta R/R)_{\text{Lorentz}}$  is approximately independent of temperature [see relation (9)]. From these assumptions, we deduce the weak-localization component to the magnetoresistance via relation (7) for the P100, VSC25, P100-4, and P120 fibers. Figure 5 shows a semilogarithmic plot of the magnetic field dependence of  $(\Delta R/R)_{\text{expt}} - (\Delta R/R)_{\text{Lorentz}}$  at various temperatures for the P100, VSC25, P120, and BDF2000 fiber samples.

Next, we analyze these curves in detail using the weak-localization relations (2)–(5). Here it is assumed that  $H_0 \gg H_i, H_s, H_{s.o.}$ . At low temperature, no positive magnetoresistance appears in the low magnetic field range whatever the sample considered. This means that spin-orbit coupling is negligible in our samples. So, in the fitting procedure, we may set  $H_{s.o.} = 0$  at each temperature. There are three fitting parameters  $H_i$ ,  $H_s$ , and  $R_{\square} = 1/G_0$  in the theoretical formula of the magnetoresistance. Among these,  $H_i$  is temperature dependent while  $H_s$  and  $R_{\square}$  are two parameters independent of temperature. The weak-localization relations, containing these three adjustable parameters, are introduced under the integral in Eq. (6), in order to take into account the orientation of the graphite layers with respect to the magnetic field. The fit was carried out using the usual least-squares method.

The solid lines of Fig. 5 represent the best fits to the negative magnetoresistance at various temperatures and over a wide magnetic field range for the P100, VSC25, P120, and BDF2000 samples. The result of this fit is quite convincing, since it accounts for the temperature and magnetic field dependences of the negative magnetoresistance very well. For the P100-4 and P120 fibers, the simulation of the magnetoresistance data has been restricted to magnetic fields lower than 0.6 T, since for these samples Shubnikov-de Haas oscillations are already present above 1 T,<sup>9</sup> thus complicating to a great extent the analysis of the experimental data. The values of the temperature-independent adjustable parameters— $R_{\square}$  and  $H_s$ —are given in Table II for each sample. The temperature-dependent parameter related to inelastic scattering is found to take the following form:  $H_i = \alpha T^{\beta}$ . Values of  $\alpha$  and  $\beta$  are also given in Table II.

In Fig. 6 we present the temperature dependence of  $H_i$  between 20 and 200 K: a quasilinear dependence on temperature is found over a decade of temperature. A somewhat surprising result is that the values of  $H_i$  are not significantly different from one sample to another. Using relation (3) it is possible in principle to estimate the values of the inelastic scattering time  $\tau_i$  at each temperature. However, a difficulty in our case is that the diffusion constant  $D$  is not a well defined quantity, since according to relation (4), it is a function of both  $v_F$  and  $\tau_0$

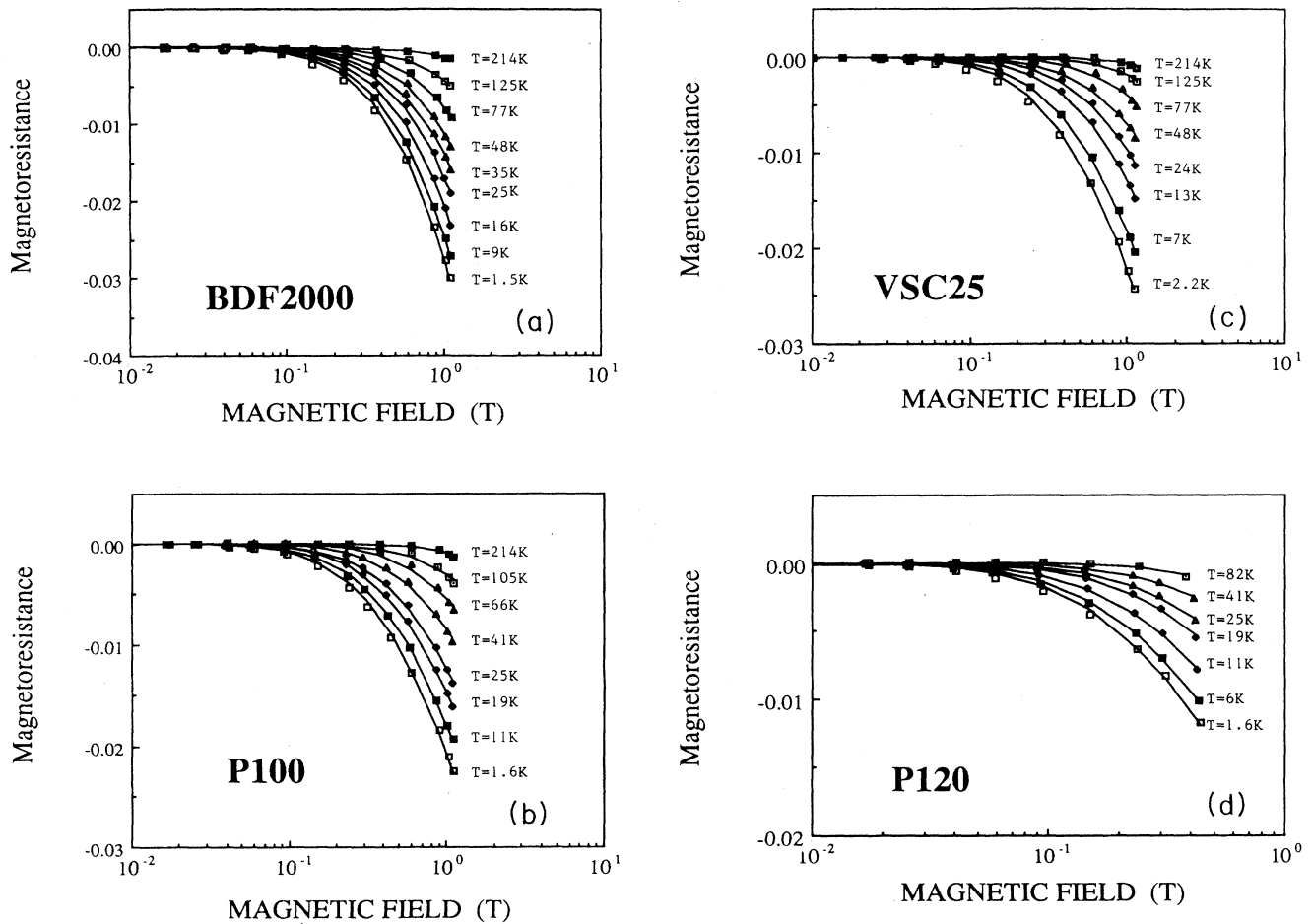


FIG. 5. Magnetoresistance vs magnetic field at different temperatures for the samples BDF2000, VSC25, P100, and P120, as indicated. The symbols correspond to the subtraction of the classical positive component of the magnetoresistance from the total measured magnetoresistance, as described in the text. The solid lines are the fits using weak-localization-theory expressions (2)–(5) and parameters given in Table II.

which cannot be determined accurately. Nevertheless, taking characteristic values for turbostratic carbons,  $v_F \approx 10^6$  m/s and  $m^* \approx 0.012m_0$ ,<sup>7,28</sup> and using  $\tau_0 = m^* \mu_0 / e$  and  $\mu_0$  as estimated from the positive component to the magnetoresistance [relation (8), with  $\mu = \mu_0$ ], a rough estimation of  $D$  can be obtained. For the

TABLE II. Parameters found by the fitting of the magnetoresistance data.

	$R_{\square}$ ( $\Omega/\square$ )	$\alpha$ ( $10^{-3}$ T/K)	$\beta$	$H_s$ ( $10^{-2}$ T)
GY-70	1573	3.70	$\approx 1$	24.2
BDF2000	3683	2.72	0.97	23.0
P55	2726	2.59	$\approx 1$	26.5
P100	2072	2.31	0.98	13.4
VSC25	2251	2.96	0.99	14.2
P100-4	1013	2.72	0.94	5.6
P120	1395	2.30	0.95	6.1

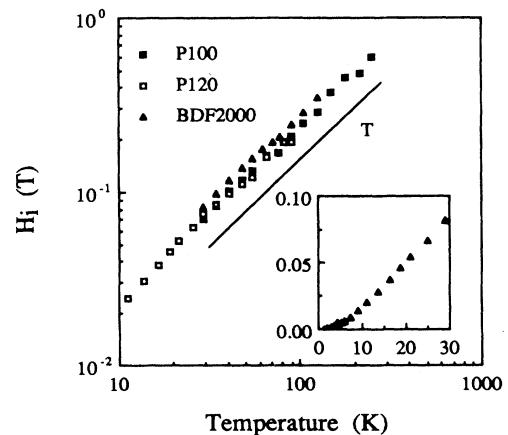


FIG. 6. Inelastic characteristic magnetic field  $H_i$  as a function of temperature for different samples, as indicated. The solid line corresponds to a linear temperature dependence. The inset to Fig. 6 shows the low-temperature variation of  $H_i$  for the BDF2000 sample.

VSC25 sample we find  $\tau_0 \approx 8 \times 10^{-15}$  s and  $D \approx 4 \times 10^{-3}$  m<sup>2</sup>/s. This leads to a room-temperature value for  $\tau_i$  of  $6 \times 10^{-14}$  s. According to relation (3), the linear temperature dependence of  $H_i$  implies that  $1/\tau_i$  follows the same dependence if only the Fermi velocity does not vary with temperature. In the framework of the STB model, this should be true only in the low-temperature range where  $k_B T \ll \varepsilon_F$ . We note that, using a weak-localization approach for the interpretation of magnetoresistance results obtained on PAN fibers, Brandt *et al.*<sup>16</sup> also found a linear temperature dependence for the inverse of the inelastic lifetime. According to the low effective temperature for electron-phonon interaction in graphite ( $\theta_D^* = 2k_F v_S h / k_B \approx 40$  K),<sup>33</sup> the physical origin of the linear temperature dependence in the temperature range 20–200 K should be the carrier-phonon interaction. The inset to Fig. 6 shows that below 20 K,  $H_i$  varies more rapidly with temperature, supporting a dominant carrier-phonon interaction as the inelastic scattering process.

Moreover, we find quantitative agreement between the inelastic-scattering-time estimation based on the weak-localization approach and that inferred from transport measurements on highly graphitized structures. Indeed, using  $\mu_i(300 \text{ K}) \approx 1 \text{ m}^2/\text{V s}$  as a typical value for single-crystal graphite or highly oriented pyrolytic graphite (HOPG),<sup>31,34</sup> we find  $\tau_{i \text{ transp}}(300 \text{ K}) \approx 7 \times 10^{-14}$  s using the same value as given above for the effective mass. However, it should be stressed that the inelastic scattering that enters into the theories relevant to weak localization may, in principle, differ from the inelastic scattering that causes the ideal resistivity. Indeed, they should be equal only if all inelastic-scattering events contribute to the resistance and if there is no restriction on small scattering angles.

The weak-localization relations (2)–(5) hold only in the weakly disordered regime where the product  $k_F l_0$  ( $k_F$  is the Fermi wave vector and  $l_0$  is the carrier mean free path) is higher than unity. If  $k_F l_0$  is very close to 1, higher-order terms in the perturbation treatment of the localization theory<sup>21</sup> can have a significant effect. For our pregraphitic fibers, these relations may be applicable because the value of  $k_F l_0$  is roughly estimated between 1 and 5 from the above values given for  $v_F$  and  $\tau_0$ .

For a metal film, the sheet resistance is usually defined as the bulk resistivity  $\rho$  divided by the thickness of the film  $d$ , i.e.,  $R_{\square} = \rho/d$ . In our samples, the ratio  $\rho/R_{\square}$  takes values between 15 and 40 Å. We note that these values are about 1 order of magnitude lower than the crystallites size along the  $c$  direction  $L_c$ ,<sup>28</sup> though the physical meaning of this parameter is still not clear.

The parameter  $H_s$  is due to the presence of magnetic impurities in the graphite fibers. It has been demonstrated that a few ppm of magnetic impurities was sufficient to make the magnetic-scattering time comparable to the inelastic-scattering time.<sup>18</sup> According to the growth processes of carbon fibers,<sup>35</sup> magnetic impurities may be present in small quantities in our samples, though most of the impurity atoms are driven out during the heat-treatment process.

In addition, it must be noted that the negative temperature coefficient of the resistivity observed in the low-temperature range and the negative magnetoresistance cannot be attributed to the Kondo effect. Indeed, in the temperature range considered, there are no anomalies typical of the Kondo effect in thermoelectric power, which depends linearly on the temperature for the pregraphitic samples investigated here.

## V. CONCLUSIONS

We have performed resistance and magnetoresistance measurements on a set of pregraphitic carbon fibers from room temperature down to 1.5 K. All the samples exhibit anomalous negative-temperature coefficients of the zero-field resistivity in the liquid-helium temperature range, in disagreement with the STB model predictions for the charge-carrier variation. Transverse applied magnetic fields tend to suppress this anomalous behavior so that for a sufficiently large magnetic field, the resistivity becomes nearly temperature independent. This result indicates that the negative magnetoresistance originates from the suppression of an additional temperature-dependent resistivity mechanism, rather than from a field-induced increase in the carrier density, as proposed in the Bright model. This additional resistivity, as well as the magnetoresistance value, increase with decreasing temperature.

Next, we have shown that the 2D weak-localization phenomenon gives a quantitative description of the temperature and magnetic field dependences of the negative magnetoresistance over a wide temperature range. A comparison of the experimental magnetoresistance data obtained at different temperatures makes it possible to determine the relaxation times that characterize the weak-localization phenomenon. A significant outcome of this work is the understanding of the inelastic scattering that destroys the phase coherence which is essential for the weak-localization phenomenon. From our magnetoresistance measurements, we have identified the electron-phonon scattering as an essential factor in the inelastic mechanisms. In addition, we find good agreement between the values of the inelastic-scattering time determined from our localization approach and those found directly from transport measurements.

We note finally that the 2D weak-localization phenomenon is a 2D quantum diffusion effect, which does not require knowledge of the band structure, as is the case in the Bright approach.

## ACKNOWLEDGMENTS

The authors are indebted to Professor M. S. Dresselhaus and Dr. G. Dresselhaus for critical reading of the manuscript and pertinent suggestions, and for providing the heat-treated BDF sample. We also thank Dr. R. Bacon and Dr. L. Singer for providing the high-modulus mesophase pitch-based fibers and Dr. J. Naud for the x-ray diffraction measurements. One of us (V.B.) was supported by a grant from the Institut pour l'Encouragement de la Recherche dans l'Industrie et l'Agriculture (Brussels, Belgium).

- <sup>1</sup>S. Mrozowski and A. Chaberski, *Phys. Rev.* **104**, 74 (1956).
- <sup>2</sup>L. C. Blackman, G. Saunders, and A. R. Ubbelohde, *Proc. R. Soc. London, Ser. A* **264**, 19 (1961).
- <sup>3</sup>G. A. Saunders, *Appl. Phys. Lett.* **4**, 138 (1964).
- <sup>4</sup>K. Yazawa, *J. Phys. Soc. Jpn.* **26**, 1407 (1969).
- <sup>5</sup>Y. Hishiyama, *Carbon* **8**, 259 (1969).
- <sup>6</sup>P. Delhaes, P. de Kepper, and M. Uhlrich, *Philos. Mag.* **29**, 1301 (1974).
- <sup>7</sup>I. L. Spain, K. J. Volin, H. A. Goldberg, and I. Kalnin, *J. Phys. Chem. Solids* **44**, 839 (1983).
- <sup>8</sup>A. A. Bright and L. S. Singer, *Carbon* **17**, 59 (1979).
- <sup>9</sup>L. D. Woolf, H. Ikezi, and Y. R. Lin-Liu, *Solid State Commun.* **54**, 49 (1985).
- <sup>10</sup>P. D. Hamburger, *Appl. Phys. Commun.* **5**(4), 223 (1985).
- <sup>11</sup>M. Endo, Y. Hishiyama, and T. Koyama, *J. Phys. D* **15**, 353 (1982).
- <sup>12</sup>I. Rahim, K. Sugihara, M. S. Dresselhaus, and J. Heremans, *Carbon* **24**, 663 (1986).
- <sup>13</sup>A. A. Bright, *Phys. Rev. B* **20**, 5142 (1979).
- <sup>14</sup>K. Sugihara and M. S. Dresselhaus, *Extended Abstracts of the 1986 Materials Research Society Symposium on Graphite Intercalation Compounds, Boston*, edited by M. S. Dresselhaus, G. Dresselhaus, and S. A. Solin (MRS, Pittsburgh, 1986), p. 35.
- <sup>15</sup>Y. Koike, S. Morita, T. Nakanomyo, and T. Fukase, *J. Phys. Soc. Jpn.* **54**, 713 (1985).
- <sup>16</sup>N. B. Brandt, V. A. Kul'bachinskii, O. M. Nikitina, and S. M. Chudinov, *Fiz. Tverd. Tela (Leningrad)* **29**, 263 (1987) [*Sov. Phys.—Solid State* **29**(1), 151 (1987)].
- <sup>17</sup>E. Abrahams, P. W. Anderson, D. C. Licciardello, and T. V. Ramakrishnan, *Phys. Rev. Lett.* **42**, 613 (1979).
- <sup>18</sup>G. Bergmann, *Phys. Rep.* **107**, 1 (1984).
- <sup>19</sup>S. Hikami, A. I. Larkin, and Y. Nagaoka, *Prog. Theor. Phys.* **63**, 707 (1980).
- <sup>20</sup>D. Rainer and G. Bergmann, *Phys. Rev. B* **32**, 3522 (1985).
- <sup>21</sup>P. A. Lee and T. V. Ramakrishnan, *Rev. Mod. Phys.* **57**, 287 (1985).
- <sup>22</sup>*Localization, Interaction and Transport Phenomena*, Vol. 61 of *Springer Series in Solid-State Sciences*, edited by B. Kramer, G. Bergmann, and Y. Bruynseraede (Springer-Verlag, Berlin, 1985).
- <sup>23</sup>L. Piraux, J.-P. Issi, J.-P. Michenaud, E. McRae, and J. F. Maréché, *Solid State Commun.* **56**, 567 (1985).
- <sup>24</sup>L. Piraux, V. Bayot, J.-P. Michenaud, J.-P. Issi, J. F. Maréché, and E. McRae, *Solid State Commun.* **59**, 711 (1986).
- <sup>25</sup>L. Piraux, V. Bayot, X. Gonze, J.-P. Michenaud, and J.-P. Issi, *Phys. Rev. B* **36**, 9045 (1987).
- <sup>26</sup>A. Klein, *J. Appl. Phys.* **35**, 2947 (1964).
- <sup>27</sup>J. Heremans, *Carbon* **23**, 431 (1985).
- <sup>28</sup>M. S. Dresselhaus, G. Dresselhaus, K. Sugihara, I. L. Spain, and H. A. Goldberg, in *Graphite Fibers and Filaments*, Vol. 5 of *Springer Series in Materials Science*, edited by M. Cardona (Springer-Verlag, Berlin, 1988).
- <sup>29</sup>M. Endo, *J. Mater. Sci.* **23**, 598 (1988).
- <sup>30</sup>T. C. Chieu, G. Timp, M. S. Dresselhaus, M. Endo, and A. W. Moore, *Phys. Rev. B* **27**, 3686 (1983).
- <sup>31</sup>L. D. Woolf, J. Chin, Y. R. Lin-Liu, and H. Ikezi, *Phys. Rev. B* **30**, 861 (1984).
- <sup>32</sup>R. Rosenbaum, *Phys. Rev. B* **32**, 2190 (1985).
- <sup>33</sup>D. T. Morelli and C. Uher, *Phys. Rev. B* **30**, 1080 (1984).
- <sup>34</sup>I. L. Spain, in *Chemistry and Physics of Carbon*, edited by P. L. Walker, Jr. and P. A. Thrower (Dekker, New York, 1981), Vol. 16, p. 143.
- <sup>35</sup>A. Oberlin, M. Endo, and T. Koyama, *J. Cryst. Growth* **32**, 335 (1976).